Egyptian Geophysical Society
EGS Journal, Vol. 19, No. 1, 119-133 (2021)

FACIES ANALYSIS AND RESERVOIR ROCK TYPING OF THE LOWER ABU MADI RESERVOIR IN WEST EL MANZALA FIELD, ONSHORE NILE DELTA, EGYPT

M.F. ABU-HASHISH[(1)], *N.M. HASSAN*[(1)], *and A.W. AL SHAREIF*[(2)]

(1) Department of Geology, Faculty of Science, Menoufia University, El Menoufia, Egypt.
(2) El Wastani Petroleum Company (WASCO), 5th Settlement, New Cairo, Egypt.

تحليل السحنات الصخرية و التصنيف النوعي لصخور خزان أبو ماضي السفلي في حقل غرب المنزلة، دلتا النيل البرية، مصر

الخلاصة: تعد عملية تحليل السحنات الصخرية و التصنيف النوعي للصخور بمثابة دراسات مهمة لفهم التفاصيل الدقيقة لخزان الرمال الطيني الصخري في دلتا النيل.

التصنيف النوعي للصخور هو طريقة تقسيم صخور الخزان إلى وحدات تدفق تبعا لتوزيع المسارات المسامية وأداء التدفق، تحليل السحنات الصخرية يمكننا حسابه من تحليل العينات اللبية الأسطوانية التي تعد الطريقة المباشرة لتحديد خصائص صخور الخزان و التي سبق الحصول عليها من العينات الأساسية في الجزء المراد دراسته.

يعد خزان ميسينيان أبو ماضي الصخري أول وأهم اكتشاف للغاز في دلتا النيل البرية، وبالتالي فإن خزان أبو ماضي السفلي في حقل غرب المنزلة والذي يقع في الجزء الشرقي من شرق دلتا النيل على الساحل الغربي لبحيرة المنزلة ويمثل فرع شرق دمياط, مثالًا عمليا لتأثيرات تغيرات السحنات الصخرية والمعايير البتروفيزيائية المختلفة في الخزان الصخري الرملي الطيني في منطقة دلتا النيل، و التي تؤدي إلى مساهمة متداخلة معقدة من وحدات الخزان في الإنتاج دون التمييز بين هذه الوحدات المختلفة في نفس الخزان المنتج.

وفقًا لنتائج التصنيف النوعي للعينات الصخرية لخزان أبو ماضي السفلي في حقل غرب المنزلة، يمكن فصل الصخور المنتجة المنتجة لخزان أبو ماضي السفلي إلى ثلاثة وحدات رئيسية, و هم: جيدة , معتدلة و منخفضة وذلك وفقًا لجودة خصائص الخزان الصخري وتحديد وحدات التدفق الهيدروليكي، و بناءا علي هذا التصنيف يمكن أن يتم تتبع أفضل وحدة تدفق لها أعلي إنتاجية و التي تتميز بأفضل الخصائص الصخرية, مما يؤدي إلى زيادة إنتاجية خزان الغاز الرمل الطفلى ميسينيان أبو ماضي في دلتا النيل البرية.

ABSTRACT: *Facies analysis and reservoir rock typing studies are essential requirement for accurately understanding the performance and properties of the shaly sand reservoir challenge in the Nile Delta.*

Reservoir rock typing is a method for reservoir rock classification into flow units with uniform pore throat distribution and flow performance. Core analysis is the direct method to measurement of the reservoir rock properties. Facies Analysis is interpreted from core data.

The Messinian Abu Madi clastic reservoir represents the first and great significant gas discovery in the onshore Nile Delta, the South Faraskour-3 well is representative of Lower Abu Madi reservoir in West El Manzala field, which is located in the eastern part of East Nile Delta Onshore at the western edge of El Manzala Lake and east of the Damietta branch. It is representing an executive example of the facies changes effect and various rock parameters in a shaly sand clastic reservoir in the Nile Delta area, which produces complex overlapping contribution in the production without distinguishing between these different units in the same productive reservoir.

According to this rock typing analysis results the Lower Abu Madi (LAM) productive reservoir can be segregated into three units: good, moderate and low according to quality of rock reservoir parameters and delineation of flow units. By tracing the facies which has the best flow performance along all the gas field reservoirs, leading to increase the productivity of the shaly sand Messinian gas reservoir of the Onshore Nile Delta.

1. INTRODUCTION

The Nile Delta is one of the main hydrocarbon provinces in Egypt. It has a significant sharing in the Egyptian national production and represents the Egypt's promising future in the field of hydrocarbon production proven by huge recent gas discoveries like Zohr gas field, which covers the internal needs of the natural gas, and enables Egypt to become one of the largest gas exporters in the Middle East.

Due to the fact that the reservoirs of the Nile Delta are of stratigraphic trap type, it contains high amount of clay minerals which affect the accuracy of the petrophysical evaluation and reservoir calculation leading to inaccuracy in the hydrocarbon reserve estimation, so that the reservoir characterization has to be implemented in such shaly sand reservoirs with high degree of facies changes.

West El Manzala field is located in the eastern part of the Nile Delta Onshore, at the western edge of El Manzala Lake, and east of the Domeitta Nile branch. It lies between the latitudes 31º 41' N, 31º 21' N and the longitudes 31º 42’ E, 31º 48’ E.

An index map showing Regional Map of Nile Delta and Location Map of Study area with well location of West El Manzala development lease covering about 82.2 km² is given in Fig. 1.

Geologic Setting

The database comes from the West El Manzala gas field located at the eastern part of onshore Nile Delta, (Fig. 1). During the Messinian age (from 7.24 to 5.33 My), the Mediterranean was isolated gradually from the Atlantic Ocean, leading to the wide extension precipitation of gypsum (from 5.96 to 5.6 My), massive salt deposition (from 5.6 to 5.5 My), and a sudden falling in sea level, followed by the creation of brackish water environments from “Lago-Mare” (Lake Sea) facies (Roveri et al., 2014). This sea level severe drop caused a huge fall in Mediterranean Sea water level, which is followed by wide erosion and the formation of large canyons incisions expanded around the Mediterranean, in addition to the spreading of salt deposits in the depocenter of the basin (Dolson et al., 2005). The Mediterranean's Messinian salinity crisis triggered the development of 5 major Paleo-drainage systems along the northern coastline of Egypt. The major canyons were filled with deposits of Qawasim and Abu Madi Fm. (Pigott and Abdel-Fattah, 2014). The interval of interest is the Upper Messinian Abu Madi Formation that occurs approximately 2600–3000 meters below the surface, and it gets a thickness of 100m. The type section of Abu Madi Formation is the Abu Madi -1 well, the Abu Madi Formation was uncomfortably overlain the Sidi Salem Formation. However, the base of the Abu Madi Formation (top of the Qawasim Formation) was generally defined by a local unconformity. In other localities, it was conformable overlain the Qawasim Formation and was conformably overlain by the Kafr El Sheikh Formation (Issawi et al., 1999). The majority of gas fields in Nile Delta had been produced from Abu Madi Formation (Schlumberger, 1984). These sandstone reservoirs were considered as the main gas producing horizons in the Nile Delta area. (Figs. 2 to 4). At the start of the Pliocene, a great sea transgression has flooded the all of the Nile Delta basin, producing Kafr El Sheikh Formation, which characterized by the deposition of thick marine shales with thin layers of interbedded sandstones. A sudden sea level drops at the early Pleistocene age leaded to the deposition of El Wastani Formation, which is a low stand deltaic system to shelf-margin deposits. Abu Madi Formation is subdivided in two informal members, upper Abu Madi Member and the lower Abu Madi Member. Oligocene - Neogene stratigraphic succession within the Nile Delta area represented by El Heiny, Enani; (1996) and Vandre´et al.; (2007) as the following Nile Delta Stratigraphic classification:

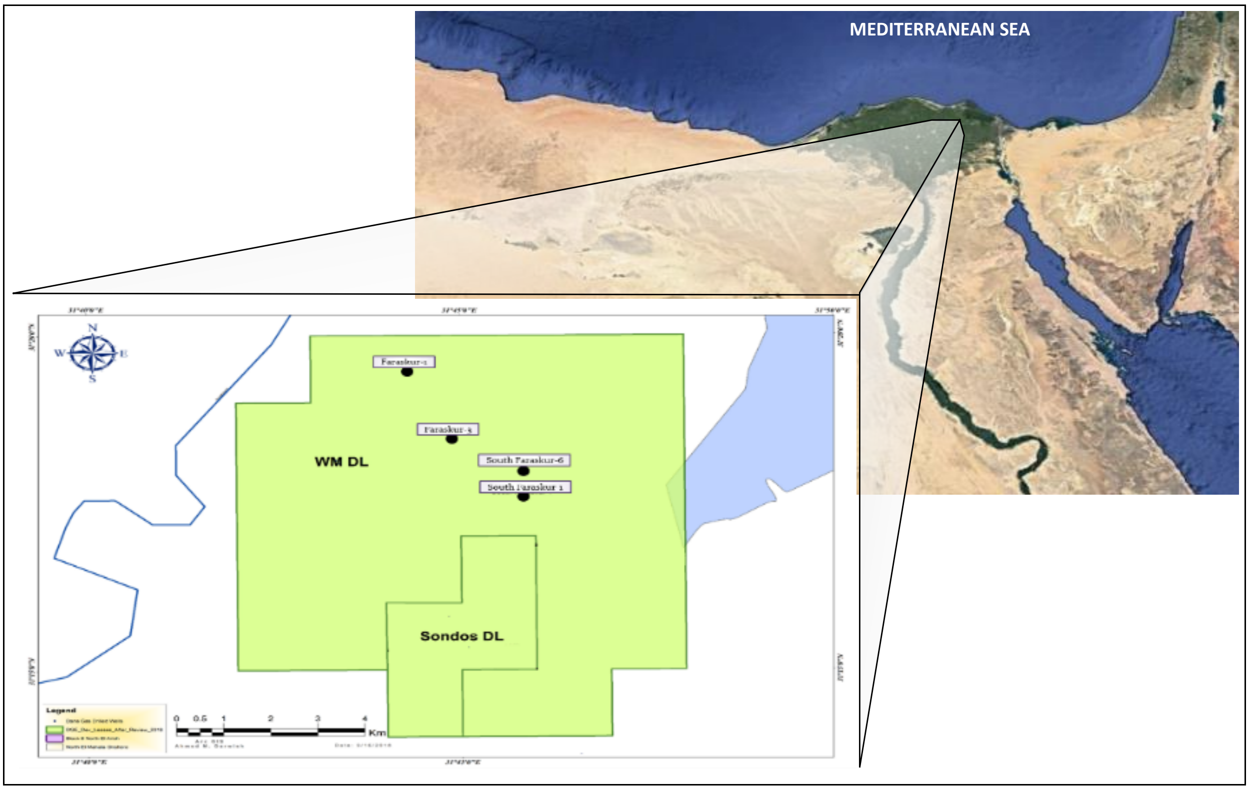

Fig. 1: Location of West El Manzala development lease, onshore East Nile Delta.

Kafr El Sheikh Formation	Early to late Pliocene
Abu Madi Formation	Messinian
Qawasim Formation	Messinian
Sidi Salem Formation	Serravallian-Tortonian
Qantara Formation	Burdigalian-Langhian
Tineh Formation	Oligocene- Aquitania

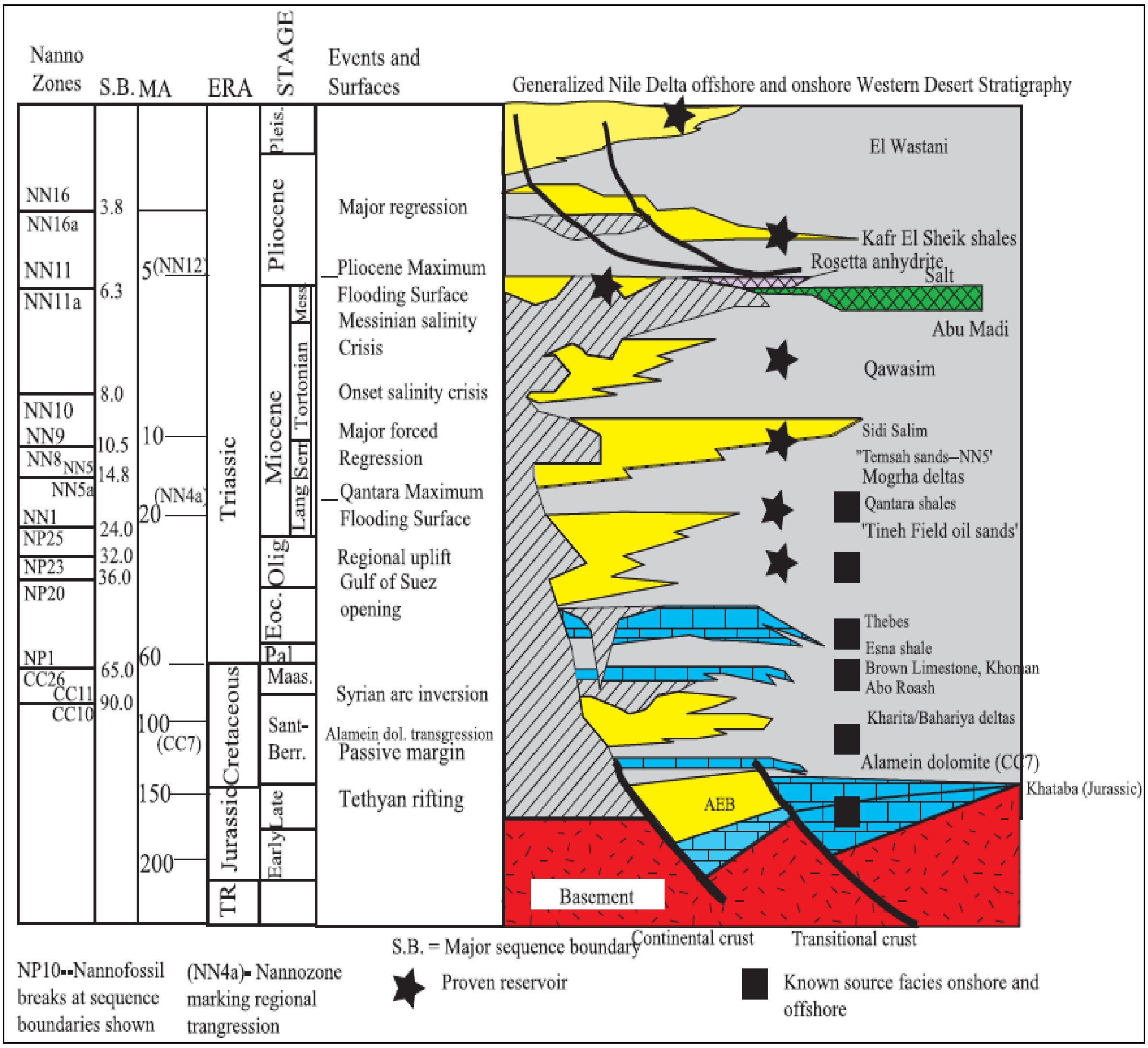

Fig. 2: Nile Delta tectono stratigraphic column. The diagram represents onshore to offshore stratigraphy from the Western Desert to the deep water Nile Delta. Nannofossil assemblages shown are at key flooding surfaces and unconformities. (After Dolson et al., 2005).

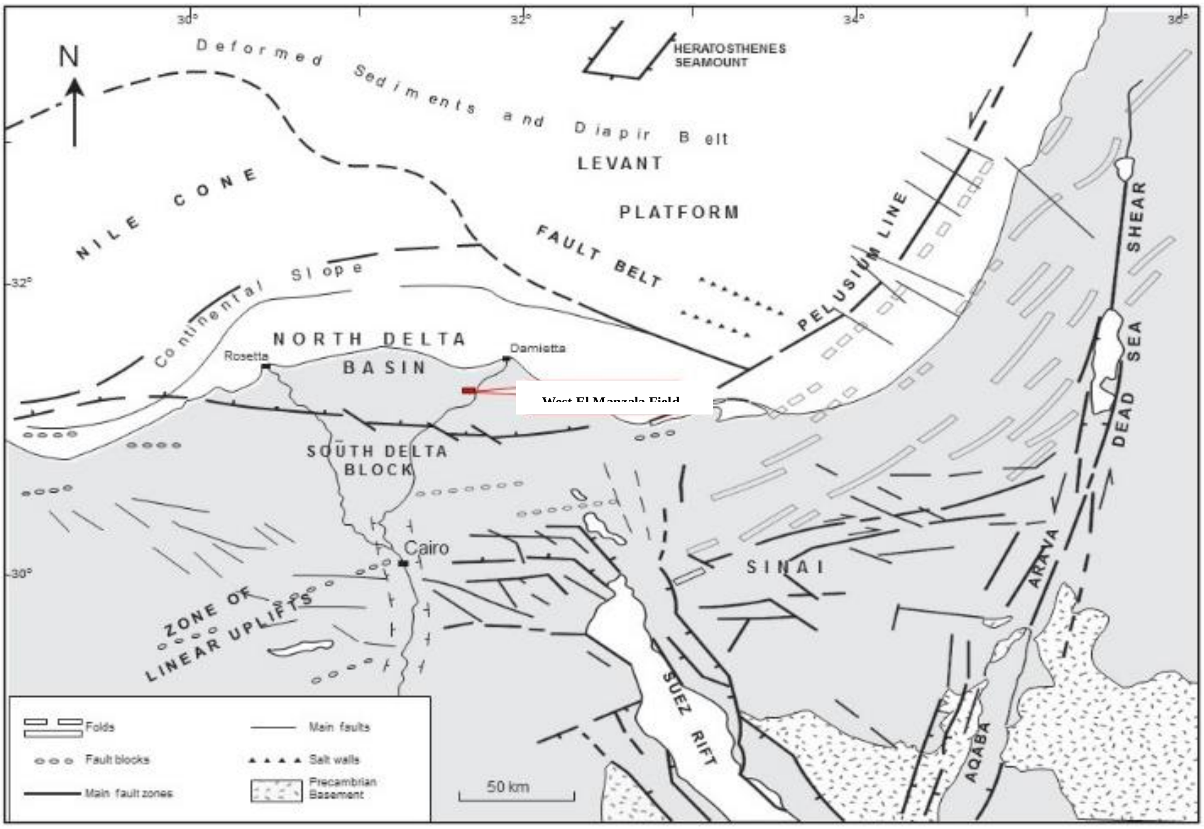

Fig. 3: Main tectonic features of the Nile Delta, Sinai and southeast Mediterranean region (after Sestini, 1989).

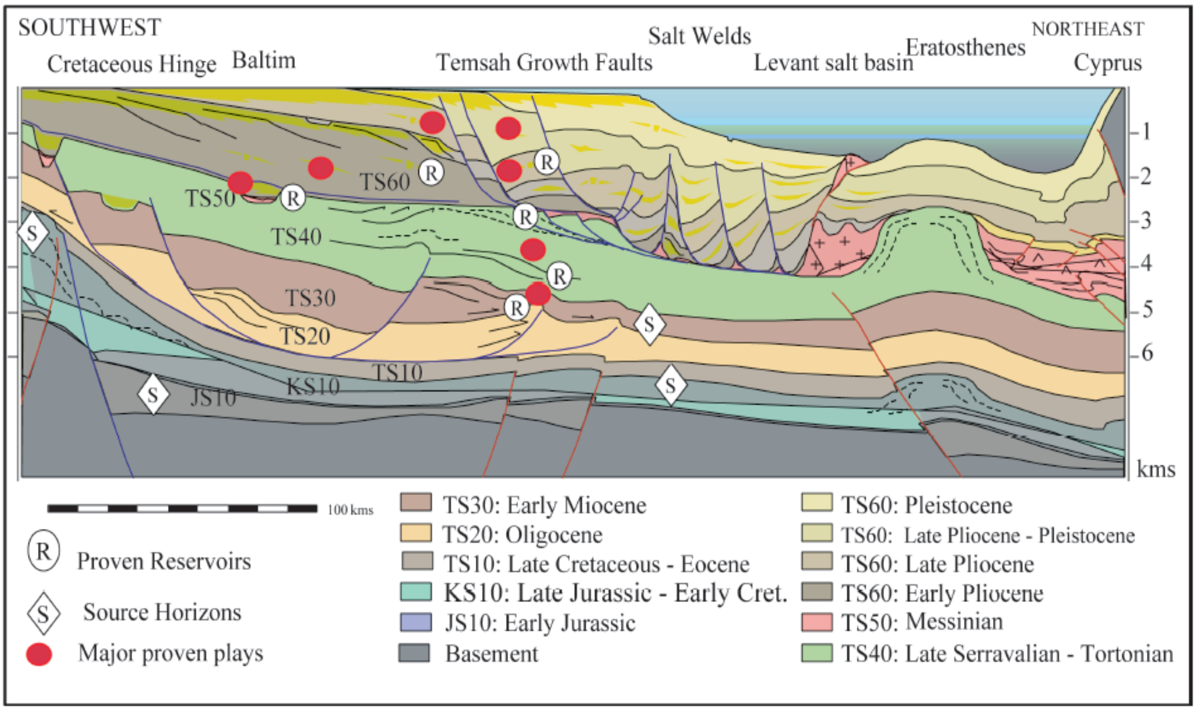

Fig. 4: Schematic diagram of Nile Delta stratigraphy and structure. Modified from Dolson et al. (2001); Deep source rocks generate hydrocarbons which have migrated as high as the Pleistocene in some fields. Biogenic gas is also common in the shallower section. (Dolson et al., 2005).

Biostratigraphically, the Messinian succession is mainly lacking marine Foraminifera except Ammonia Beccarii and Ostracods (Rio et al., 1990) at some horizons. On the other hand, the Messinian sequence is subdivided into Qawasim and Abu Madi formations being correlated with the two main nannoplanktonic zones; Helicosphaera Orientalis (NN11b) and Reticulofenestra Rotaria (NN11c), respectively. The Messinian deposits are regionally covered by the marine flooding of the Pliocene (5.3 my) based on isotopic stratigraphy. The Pliocene transgression is considered to be a consequence of the re-establishment of communications with the open sea. The Nile Delta region experienced rifting and extension in the Jurassic and Early Cretaceous with the development of east-west trending basins. This was followed by general thermal sagging and subsidence with shelf margin formation (Dolson et al., 2001).

During the Late Cretaceous-Miocene, the Jurassic-Early Cretaceous rift basins were inverted with the development of Syrian arc series of large northeast-southwest oriented folds south of the Nile Delta and Eastern Mediterranean regions (Darwish, 1996; Kusky, 2003). The tectono-stratigraphic evolution of the eastern Nile Delta is shown in Fig.(2). The “hinge line” (Figs. 3 and 4) is an Upper Cretaceous carbonate shelf edge that forms the southern boundary of thick Neogene sediments in the Nile Delta. It is an essential element affected the overall stratigraphic and tectonic evolution of the Nile Delta basins.

A subsequent rifting phase (Gulf of Suez rift) occurred during Oligo-Miocene with a dominant extension orientated in northwest faults due to divergence of the African plate away from the Arabian plate. The Oligo-Miocene or older E-W and NW trending faults in the Nile Delta were suggested to be related to the initial rifting phases of the Gulf of Suez (Fig. 3).

The gross seismic stratigraphic framework of the study area is described with reference to main representative seismic section, perpendicular to the depositional direction of the Messinian depositional system (Fig. 4) and summarized in the stratigraphic chart (Fig. 2).

Methodology and Data Set

This study utilizes a comprehensive approach that, segregates the Lower Abu Madi productive reservoir into specific hydraulic flow units by using core analysis data of the Lower Abu Madi reservoir in West El Manzala field. The methodology is including three steps as follows:

A) Core Data Analysis:

19.8m core has been used to represent the Lower part of the Abu Madi Formation reservoir in South Faraskour-3 well. Core analysis data are a direct method to determine the reservoir rock properties obtained from core samples at the zone of interest. Core description allows sufficient resolution to distinguish the different litho-facies and depositional elements within Lower Abu Madi reservoir. Core data has been used in rock typing analysis of the reservoir rock to classify the reservoir into flow units, and facies analysis.

Table 1: South Faraskur-3 well cut Core Results Data.

Well Name	Interval Cut (m)	Interval Recoverd (m)	Recovered (m)	Percentage Recovered	Zone
S.Faraskur-3	2818– 2837.8	2818– 2837.8	19.8	100%	Lower Abu Madi

B) Stratigraphic and structure interpretation of the Upper Messinian reservoir (Abu Madi Formation reservoir) inside the West El Manzala field, showing that the Structure is generally smooth and dipping to the Northwest direction with the seismic amplitude marking the distribution of the reservoir units within the reservoir level.

C) Facies Analysis and Rock Typing Integration:

The rock typing analysis of South Faraskour-3 well in the lower Abu Madi reservoir, Facies analysis and petrophysical parameter from the core data interpretations are essential to make an integration for clear and detailed reservoir analysis and for the delineation of hydraulic flow units which distinguishes its deposits specific facies characterization.

Abu Madi Formaion

Locality Type:

The Abu Madi Formation was introduced by the National Committee of Geology Science (NCGS) in 1974. The type section is in Abu Madi-1 located at (lat. 31° 27′ N and long. 31° 22′ E). The maximum thickness of Abu Madi Formation reached about 592 m in Kafr El Sheikh- 1 Well (depth intervals between 2738 to 3330 m).

Lithological Characteristics:

The Abu Madi Formation sediments have been described as a succession of thick layers of rarely conglomeratic sandstone and interbedded with shale layers which repeats and became thicker in the upper part of Abu Madi Fm. The sand is composed of quarzitic variable in grain size and almost loose. The conglomeratic levels in a sandy matrix in the lower part of Abu Madi Fm. display the lower unconformity. The Abu Madi reservoir proved to be the best reservoir in the Nile Delta having good porosity with average about 21%. The overwhelming of gas fields in Nile Delta had been produced from Abu Madi Formation (Schlumberger, 1984). These sandstones were considered as the main gas producing zone in the Nile Delta fields.

Faunal Content and Age:

Abu Madi Fm. stratigraphic subdivision was generally adopted, although there were some different opinions concerning its age. First definition was supposed that it was formed in early Pliocene (Rizzini et al., 1978) but more recent considerations assign it to late Miocene -Messinian (El Heiny and Enani, 1996 and Vandr et al., 2007).

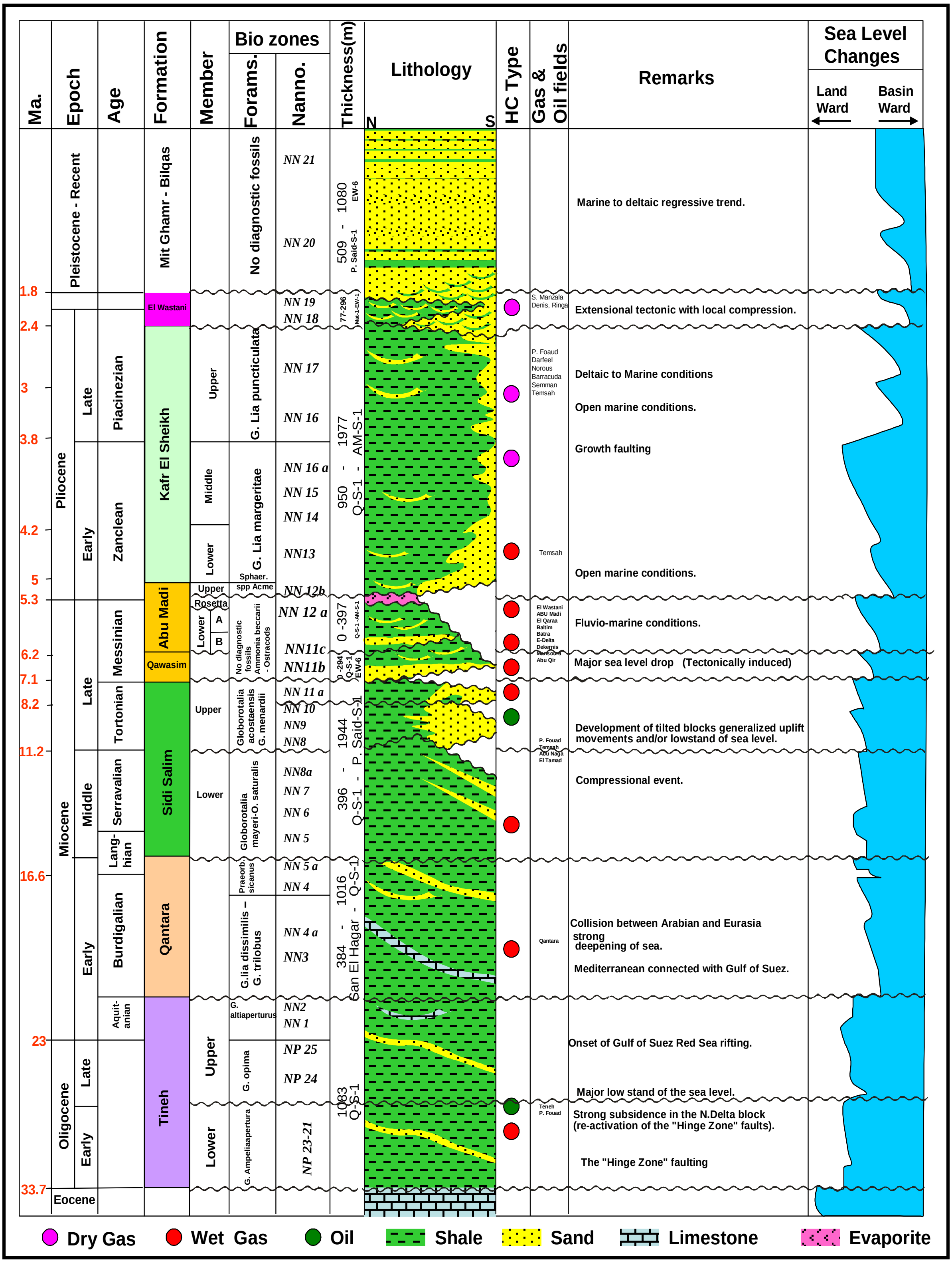

Fig. 5: West El Manzala field Generalized Stratigraphic column (after WASCO internal report, 2016).

This Formation generally contains a rare funal content of benthonic foraminifera and it is detected by the appearance of *sphaeroidinellopsis sp*. Also, Abu Madi Fm. in West El Manzala field could be detected by the appearance of NN11c Nannozone.

Boundaries:

The age of Abu Madi Fm. is a matter of controversy. In type section (Abu Madi-1 Well), Abu Madi Fm. was uncomfortably overlain the Sidi Salem Fm. However, the base of the Abu Madi Fm. (top of the Qawasim Formation) was generally defined by a local unconformity. In other localities, it was conformably overlain the Qawasim Fm. and was overlain by the Kafr El Sheikh Fm. (Issawi et al., 1999).

Depositional Environment:

This Formation was interpreted to be of fluvial to coastal marine origin and its sediments was deposited in a subsiding basin under conditions of a transgressive sea (Rizzini. et al.,.1978).

Core Analysis

The direct method to detect the rock properties in the studied reservoir is the core analysis, which was obtained from sample representing real cutting from the Lower part reservoir of the Abu Madi Formation in South Faraskour-3 well.

Table 2: South Faraskur-3 well Conventional Core Analysis Results Data.

SAMPLE NO.	DEPTH	NITROGEN PERMEABILITY (mD)		HELIUM POROSITY	HELIUM POROSITY	GRAIN DENSITY
	(m)	HORIZONTAL	VERTICAL	%	dec	gm/cm³
1	2818	442	254	27.3	0.273	2.66
2	2818.25	406	182	27.3	0.273	2.67
3	2818.5	228	291	23	0.23	2.65
4	2818.75	554	758	27	0.27	2.65
5	2819	229	122	24	0.24	2.65
6	2819.25	110	129	21.3	0.213	2.64
7	2819.5	197	87	24.8	0.248	2.64
8	2819.75	891	560	25.5	0.255	2.65
9	2820	989	932	26.8	0.268	2.65
10	2820.5	861	633	23.3	0.233	2.65
11	2820.75	93	330	26.3	0.263	2.67
12	2821	23	59	24.5	0.245	2.67
13	2821.25	43	36	23.4	0.234	2.68
14	2821.5	18	93	25	0.25	2.68
15	2821.75	60	119	24.6	0.246	2.67
16	2822	45	44	19.1	0.191	2.67
17	2822.25	92	176	20.1	0.201	2.66
18	2822.5	147	168	26.2	0.262	2.66
19	2822.75	60	88	20.4	0.204	2.65
20	2823	51	22	26.6	0.266	2.67
21	2823.25	239	134	25.5	0.255	2.65
22	2823.5	340	34	27.5	0.275	2.64
23	2823.75	129	38	24.7	0.247	2.64
24	2824	111	349	25.6	0.256	2.65
25	2824.25	320	336	30.2	0.302	2.65
26	2824.5	67	214	25.7	0.257	2.65
27	2824.75	119	185	25.7	0.257	2.65
28	2825	23	Unavailable	23.2	0.232	2.66
29	2825.25	97	63	27.6	0.276	2.66
30	2825.5	558	203	29.4	0.294	2.66
31	2825.75	6	77	14.5	0.145	2.66
32	2835.4	3.09	0.81	10.4	0.104	2.68
33	2835.9	1.93	1.04	9.5	0.095	2.67
34	2836.39	0.18	0.12	13.8	0.138	2.7

The plugs were cut with liquid nitrogen from the 2/3rd cut section. All plugs are 1-inch diameter. The 2/3rd cut sections were plugged every one foot for vertical and horizontal plugs. All samples are mounted directly after plugging. The mounted materials (Teflon Tubing and screens) were weighed to be used in permeability and porosity calculations. The core porosity analysis represents the measurement of the effective porosity, calculated from the interconnected pore volume relative to the bulk pore volume measured using helium expansion gas porosity measurement (according to Boyle's law).

Phi = pore volume/Bulk volume

The core permeability analysis determines the capacity and mobility of formation to transmit the fluids. It controls the flow rate and movement of the fluid in the reservoir. Darcy's equation is the calculation method of permeability. The Normal distributions and cumulative histograms of core porosity and permeability for the studied samples in South Faraskur-3 well are plotted in Fig.(6).

The relationship between porosity, ø, and permeability, k, are often tested for sedimentary rocks in relation to reservoir characterization and petroleum geology. A major trend of increase in permeability with porosity is normally considered. However, the effects of compaction, grain size, packing, and processes of solution or dissolution related to increase or decrease of primary and secondary porosity can produce a lot of types of relationships between different types of porosity and the permeability. From core data of South Faraskour-3 well, general relationships have been tested for a conventional core data set (33 studied samples). The permeability / porosity cross plot shown in figure 7 which shows that permeability values are directly proportional to the measured values of porosity with good correlation Coefficients.

Rock Typing

Conventional core analysis produced permeability and porosity measurements are used to determine the reservoir rock types and detect flow units of the studied samples in South Faraskur-3 well. Rock typing of the reservoir is the main process leading to reservoir classification into various flow units, with uniform pore throat distribution and flow performance for each one (Winland, 1972). Based on this flow unit classification, the real static and dynamic reservoir characters can be providing reservoir simulation model. The reservoir discrimination technique, which depends on both flow zone indicator (FZI) and reservoir quality index (RQI) which, successfully was examined and applied by many authors (e.g. Al-Dhafeeri and Nasr-El-Din2007; Othman et al. 2008; Kassab et al. 2015; etc.). The flow units in reservoir are determined using flow zone indicators (FZI) and reservoir quality index (RQI) as follows:

$$RQI=0.0314*(K/Ø)^{0.5} \quad \text{(Eq. 1)}$$

$$FZI= RQI/Øz \quad \text{(Eq. 2)}$$

$$Øz= Ø/((1-Ø)) \quad \text{(Eq. 3)}$$

where; K: Permeability md, Ø: Porosity fraction and Øz: normalized porosity.

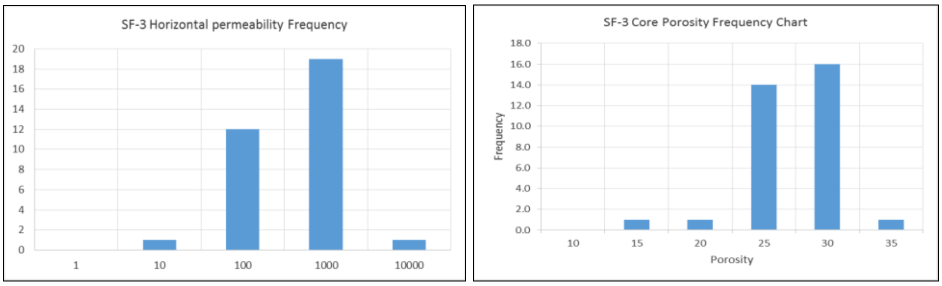

Fig. 6: Normal distributions and Cumulative plots of core porosity and horizontal permeability.

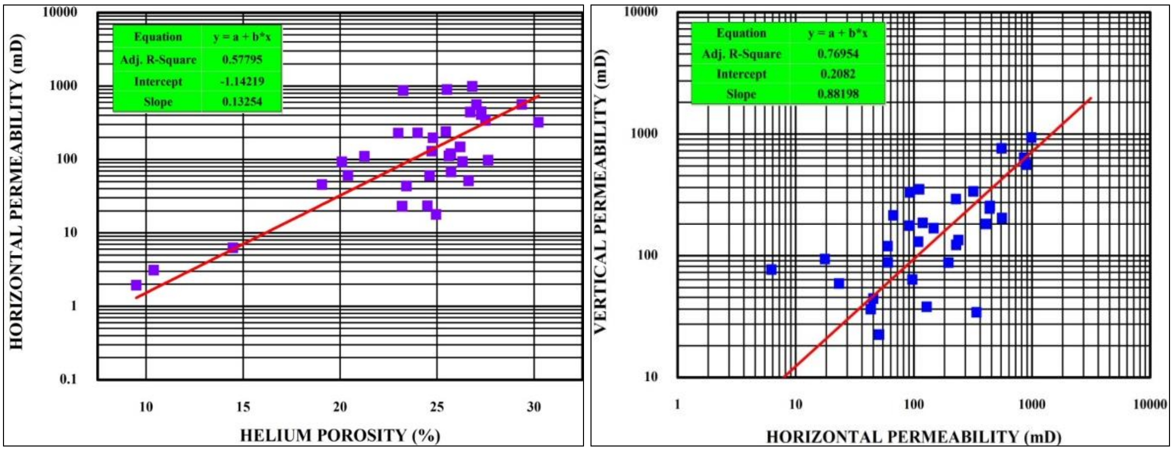

Fig. 7: Relationship plots between horizontal, vertical permeability and porosity.

Table 3: Calculation steps and the results of flow zone indicators and reservoir quality index.

0.00 Phi	Cum Phi	Cum K	RQI	Phi Norm	FZI	Predicted K (mD)
0.27	3.20	3.97	1.26	0.38	3.37	441.41
0.27	6.41	7.62	1.21	0.38	3.23	406.33
0.23	9.11	9.67	0.99	0.30	3.31	228.01
0.27	12.28	14.65	1.42	0.37	3.84	553.95
0.24	15.10	16.70	0.97	0.32	3.07	229.02
0.21	17.60	17.69	0.71	0.27	2.64	109.54
0.25	20.51	19.46	0.88	0.33	2.68	196.75
0.26	23.51	27.46	1.86	0.34	5.42	890.76
0.27	26.66	36.35	1.91	0.37	5.20	988.96
0.25	29.58	64.53	3.52	0.33	10.61	3135.75
0.23	32.32	72.26	1.91	0.30	6.30	860.50
0.26	35.41	73.10	0.59	0.36	1.65	92.85
0.25	38.28	73.31	0.31	0.32	0.94	23.32
0.23	41.03	73.70	0.43	0.31	1.40	43.33
0.25	43.97	73.85	0.26	0.33	0.79	17.68
0.25	46.86	74.39	0.49	0.33	1.50	60.10
0.19	49.10	74.80	0.48	0.24	2.06	45.49
0.20	51.46	75.63	0.67	0.25	2.67	92.18
0.26	54.53	76.96	0.74	0.35	2.10	147.40
0.20	56.93	77.50	0.54	0.26	2.11	60.36
0.27	60.06	77.96	0.43	0.36	1.20	50.91
0.25	63.05	80.10	0.96	0.34	2.81	238.60
0.28	66.28	83.15	1.10	0.38	2.91	339.47
0.25	69.18	84.31	0.72	0.33	2.18	128.85
0.26	72.19	85.31	0.65	0.34	1.90	111.21
0.30	75.74	88.18	1.02	0.43	2.36	319.48
0.26	78.76	88.78	0.51	0.35	1.46	67.14
0.26	81.78	89.85	0.68	0.35	1.95	119.19
0.23	84.51	90.06	0.31	0.30	1.03	22.97
0.28	87.75	90.94	0.59	0.38	1.54	97.34
0.29	91.20	95.95	1.37	0.42	3.29	557.88
0.14	92.91	96.00	0.21	0.17	1.22	6.23
0.27	96.04	99.95	1.27	0.36	3.49	439.35
0.10	97.26	99.98	0.17	0.12	1.47	3.09
0.10	98.38	100.00	0.14	0.10	1.35	1.93
0.14	100.00	100.00	0.04	0.16	0.22	0.18

By plotting the RQI as a function of FZI can be used as a tool for ranking the quality of the reservoir samples (El Sharawy and Nabawy 2016). The RQI / FZI cross plot in the following figure shows that the RQI values are directly proportional to FZI values with very good correlation coefficients of 0.955.

The cross plots between horizontal permeability with both of RQI and FZI show that horizontal permeability values are directly proportional to the measured values of RQI and FZI good correlation coefficients with 0.64 and 0.5.

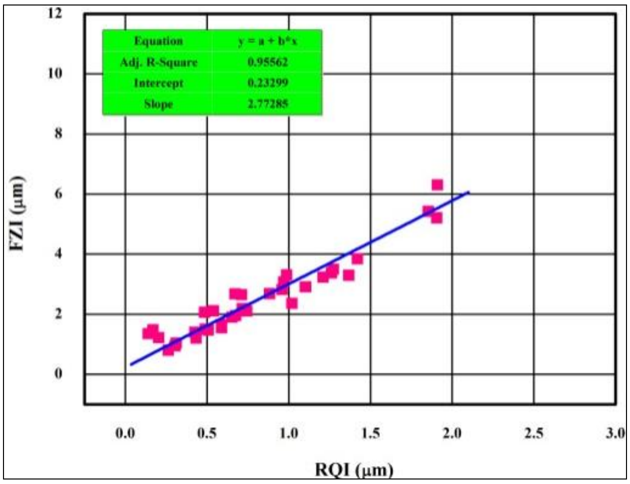

Fig. 8: Plotting RQI values as a function of FZI, taken into consideration the flow units.

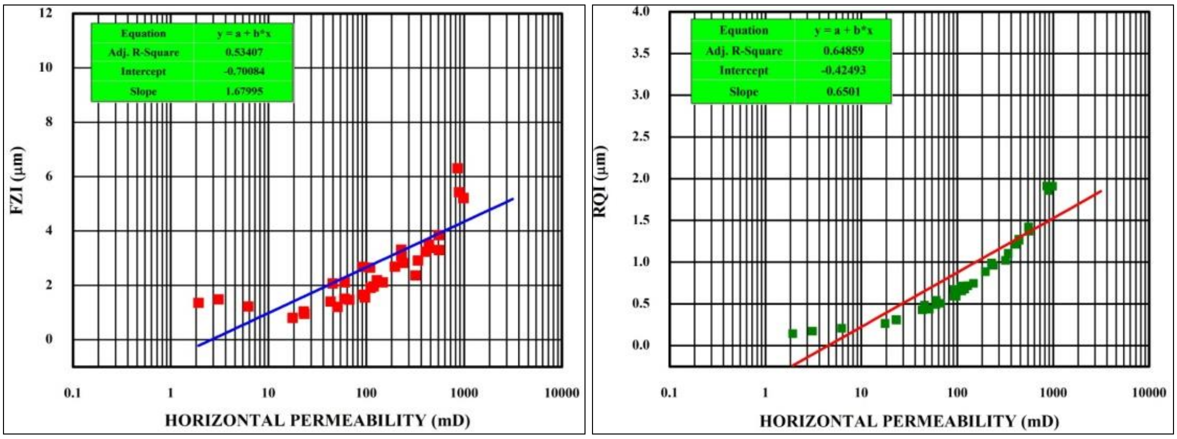

Fig. 9: permeability values measured in the horizontal direction 'kH' as function of a RQI and b FZI.

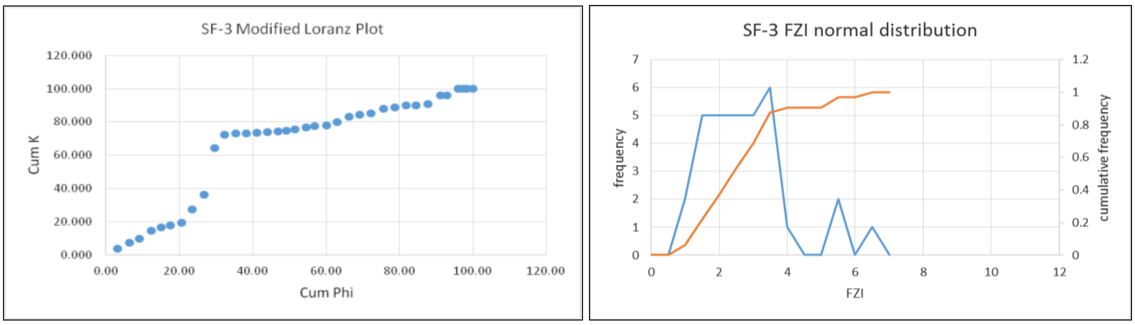

Fig. 10: Modified Loranz Plot and FZI Histogram.

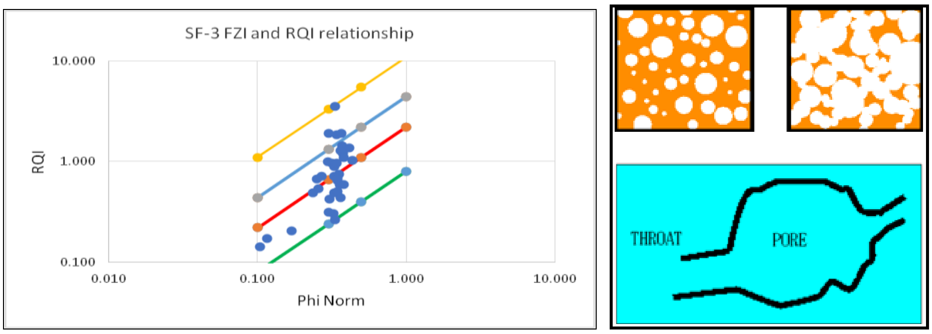

Fig. 11: Relationship plots between normalized porosity versus RQI.

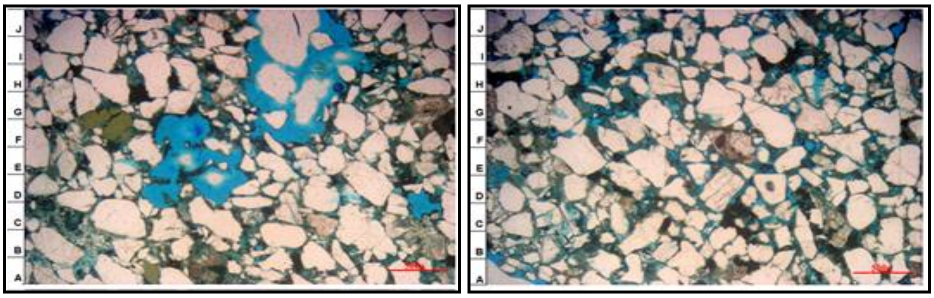

Fig.12: Thin section sample photo at depth 2824.27m.

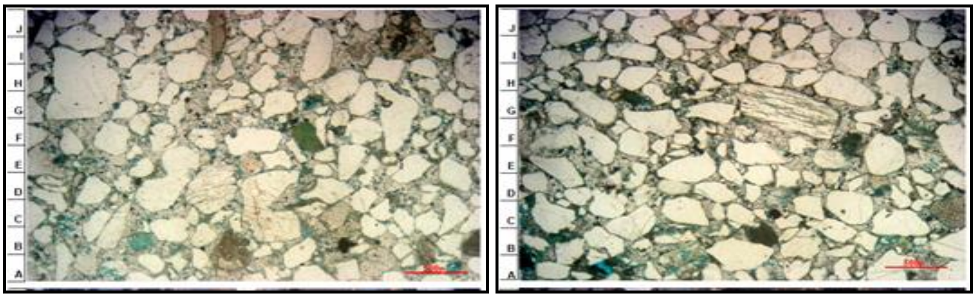

Fig.13: Thin section sample photo at depth 2825.76m.

By using Modified Loranz Plot (MLP) which based on the relation between effective porosity and horizontal permeability, every flow unit can be defined by the change of the slop of the curve as shown in figure 10. After applying Modified Loranz Plot (MLP) there are three flow units can be recognized.

The relationship between RQI and phi normalized (Øz) is used to display that samples with similar FZI values lie close together when they plot normalized porosity versus permeability on a log plot. Qualitative identification of flow units means recognition of the numbers of flow units inside the well regardless the depth and distribution of this flow units. The FZI can be measured using Eq. 2 and 3 after calculation of RQI then define FZI zones. Figure 11 illustrates the relationship plots between normalized porosity verses RQI values showing the FZI values of the samples in South Faraskur-3 well, and schematic picture detect a pore and throat in the porous material pore space, 2D picture of a) isolated circular pores, and b) connected pores.

Petrographic Analysis

The integration between flow unit analysis, the core data and petrographical characteristic is very important to obtain reservoir quality and the flow units zones interpreted and defined as three main zones:

Zone 3: average good FZI values (good quality sandstone).

Zone 2: average moderate FZI values (moderate quality sandstone).

Zone 1: average low FZI values (low quality sandstone).

The effect of grain minerals and rock properties changes on the quality of the reservoir is shown in the coming figures(12, 13 & 14) which were taken from the petrographical analysis and core report of South Faraskur -3 well Lower Abu Madi zone, (after WASCO internal report, 2011), which reflects the three types of reservoir rocks:

Quartz Arenite Litho-Facies:

Good reservoir quality zone 3 as example of depth 2824.27m with about 30% (intergranular porosity), very fine into medium grained , sub angular to rounded, well sorted, loose mature, no pore filling and grain coating detrital of clay matrix.

Feldspathic Arenite Litho-Facies:

Moderate reservoir quality zone 2 as example of depth 2825.76m with about 14% (intergranular porosity), very fine into medium-grained, sub angular to rounded, well sorted, highly cemented with carbonate, grains floating in carbonate cement, mature, abundant monocrystalline quartz grains with straight, extinction, glaucony pellets mature, microsparite carbonate.

Subfeldspathic Wacke Litho-Facies:

Low reservoir quality zone 1 as example of depth 2835.40m with about 10% (intergranular porosity), very fine into very coarse grained sand, poorly sorted, moderately cemented argillaceous matter, with point, long and floating grain contacts, abundant monocrystalline quartz grains, with attached quantities of potash feldspars are recorded. Abundant of carbonate fragments and carbonaceous debris are defined. Grain coated and pore filled by clay matrix, with poor pore interconnectivity.

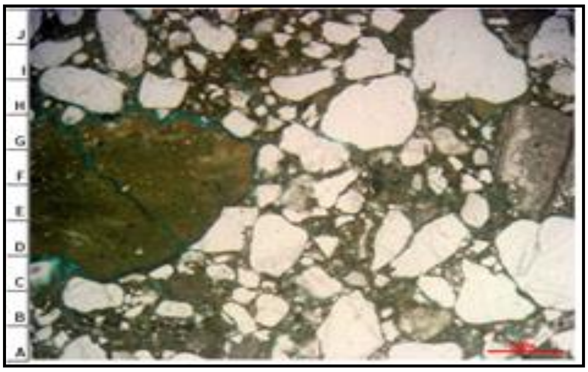

Fig. 14: thin section sample photo at depth 2835.40 m.

X-Ray Diffraction Analysis (XRD)

X-ray diffraction analysis (XRD) for clay mineral detection can explain the reason of different values of porosity, permeability and the rock quality variation. The results of the mineralogical composition that determined by XRD analysis on 5 plugs in South Faraskur-3 well are shown in Table 4.

Table 4: (XRD) results in South Faraskur-3 well.

Sample	Depth m	Sm/IL %	IL. %	Ch %	Kao %	Total Clay
1	2818.16	0	races	0	100	100
2	2825.5	3	4	0	93	100
3	2826.5	53	18	0	29	100
4	2835.1	65	4	0	31	100
5	2837.45	55	5	0	40	100

SM: Smectite, IL: Illite, CH: Chlorite, SM/IL: Smectite/Illite mixed layer, Kao: Kaolinite.

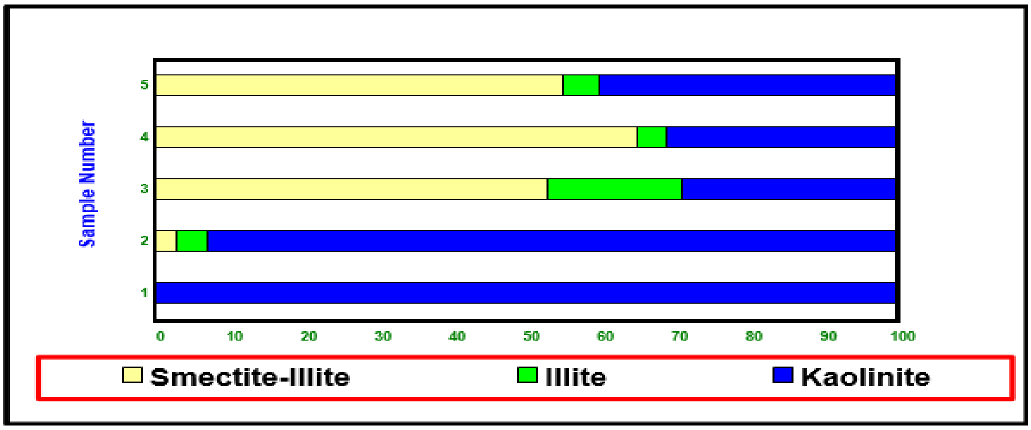

Fig. 15: Semi-Quantitative XRD Data of < 2-micron Clay Fraction (after WASCO report, 2011).

By linking the clay content per each Hydraulic Flow Unit (HFU), it is shown that, HFU-1 represented by samples number 3, 4, 5 with lowest FZI values is the highest clay content with largest amount of Smectite/illite which has very bad effect on reservoir quality and can be noticed that the values of permeability are the lowest. The highest quality rock type HFU-3 which, close to samples number 1, 2 with highest FZI values is the lowest clay content with small amount of Smectite/illite and highest permeability performance.

The results of Lower Abu Madi reservoir in South Faraskour-3 core analysis data can be summarized in figure 16 which illustrates the facies analysis and reservoir rock typing integration.

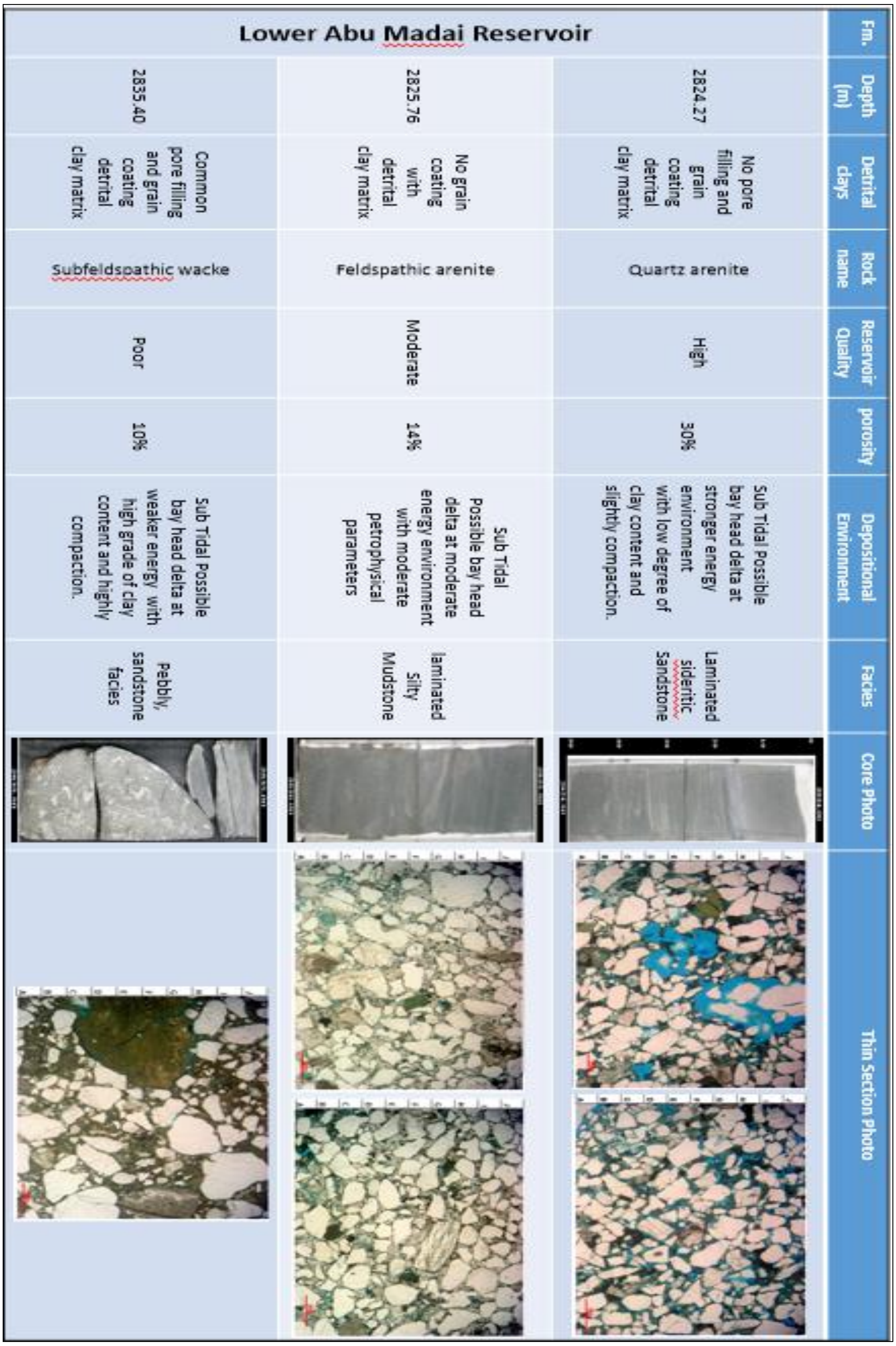

Fig. 16: Facies analysis and reservoir rock typing integration.

CONCLUSION

The sediments of the studied Abu Madi clastic reservoir core in West El Manzala field, are generally composed of three rock types of sand reservoirs with different flow performance due to a variation in clay content and the degree of compaction with depth leading to three different of hydraulic flow units as follows:

The rock type 3 with good FZI values which represents the good quality sandstone found in subtidal possible bay head delta sand deposits, which was formed in a stronger energy environment. It has the maximum porosity measured with low degree of clay content and slight compaction. The rock type 2 with moderate FZI values which represents the moderate quality sandstone found in subtidal deposits formed at moderate energy environment with moderate petrophysical parameters. The rock type 1 with low FZI values which represents the low quality sandstone found in subtidal possible bay head delta sand deposits, which was formed in weaker energy environment and have the lowest porosity measured with high grade of clay content and high compaction.

According to this rock typing analysis results and delineation of hydraulic units of flow, production can be maximized from Lower Abu Madi clastic reservoir by focusing exploration and production activities on the best flow zone with highly productive rock parameters. By tracing the facies which has the best flow performance along all the gas field reservoirs, leading to increase the productivity of the shaly sand, Messinian gas reservoir of the Onshore Nile Delta.

REFERENCES

Al-Dhafeeri, A.M., Nasr-El-Din, H.A. (2007): Characteristics of high permeability zones using core analysis, and production logging data. J.Petrol Sci and Eng 55:18–36.

Dolson, J.C., Boucher, P.J., Siok, J., Heppard, P.D. (2005): Key challenges to realizing full potential in an emerging giant gas province: Nile Delta/Mediterranean offshore, deep water, Egypt. In: Dore AG, Vining BA (ed) 6th Petroleum Geology Conference, London, United Kingdom.

Dolson, C.J.; Shaan, V.M.; Matbouly, S.; Harwood, C.; Rashed, R. and Hammouda, H. (2001): The petroleum potential of Egypt. – In: Downey, W.M.; Threet, C. J. and Morgan, A. W. (Eds.): Petroleum provinces of the twenty-first century., Memoir No. 74, p. 453-482, American Association of Petroleum Geologists, Tulsa, Oklahoma.

Dolson, J.C., Shann, M.V., Matbouly, S., Harwood, C., Rashed, R., Hammouda, H. (2001): The Petroleum Potintial of Egypt, AAPG Memoir 74, and Chapter 23 p. 453-482.

El Sharawy, M.S., Nabawy, B.S. (2016): Geological and petrophysical characterization of the Lower Senonian Matulla Formation in Southern and Central Gulf of Suez, Egypt. Arab J Sci Eng 41(1):281–300

El Heiny, I., Enani, N. (1996): Regional stratigraphic interpretation pattern of Neogene sediments, Northern Nile Delta, Egypt, E.G.P.C. 13th Exploration and Production Conference, v.1, p 270–290.

Issawi, B.; El Hinnawi, M.; Francis, M. and Mazhar, A. (1999): The Phanerozoic Geology of Egypt. A geodynamic Approach - Egypt Geol. Surv. Special Publication 76, p. 461.

Kassab, M.A., Teama, M.A., Cheadle, B.A., El-Din, E.S., Mohamed, I.F., Mesbah, M.A. (2015): Reservoir characterization of the Lower Abu Madi Formation using core analysis data: El-Wastani gas field. Egypt J Afr Earth Sci 110:116–130

Kusky, T.M., Abdelsalam, M., Tucker, R., Stern, R.J. (2003): Evolution of the East African and related Orogens, and related Orogens, and the assembly of Gondwana. Spec Issue Precambr Res 123:81–344.

Manzi, V., Lugli, S., Roveri, M., Dela Pierre, F., Gennari, F., Lozar, F., Natalicchio, M., Schreiber, B.C., Taviani, M., Turco, E. (2014): The Messinian salinity crisis in Cyprus: a further step towards a new stratigraphic framework for Eastern Mediterranean. Basin Res 1–30.

Othman, A., Nabawy, B.S., Abdel Hafeez, T., Saher, M., Abdel, K.R. (2008): Reservoir quality discrimination of the lower part of Bahariya Formation, N. Qarun Oil Field, W.D. Egypt. EGS J 6(1):81–101

Rio, D., Fornaciari E. & Raffi I. (1990): Late Oligocene through early Pleistocene calcareous nannofossils from western equatorial Indian Ocean (Leg 115). Proc. ODP, Sci Res., 115, 175-235.

Rizzini, A., Vezzani, F., Coccocetta, V., & Milad, G. (1978): Stratigraphy and Sedimentation of Neogene-Quaternary section in the Nile Delta area, Egypt - Marine geology 27: p. 327-348.

Schlumberger (1984): Well Evaluation Conference, Egypt: Geology of Egypt: p. 1-64.

Sestini, G. (1989): Nile Delta: a review of depositional environments and geological history, in Whately, M. K. G., and Pickering, K. T., eds., Deltas: sites and traps for fossil fuels: Geological Society, London, Special Publication, no. 41, p. 99-127.

Vandré, C.; Cramer, B.; Gerling, P. and Winsemann, J. (2007): Natural gas Formation in the western Nile delta (Eastern Mediterranean): Thermogenic versus microbial. - Jour. Organic Geochemistry 38: p. 523 – 539.

WASCO (2011): Integrated Study on Conventional Core samples well: South Faraskur-3 on El Wastani Petroleum Company (WASCO) West El Manzala development lease (Internal Report).

WASCO (2016): Regional study of the Upper and Lower Messinain sequence on El Wastani Petroleum company (WASCO) development leases (Internal Report).

Winland, H.D., (1972): Oil Accumulation in Response to Pore Size Changes, Weyburn Field, Saskatchewan: Amoco Production Research Report, No. F72-G-25.